

Decelerating Airy pulse propagation in highly non-instantaneous cubic media

LIFU ZHANG,^{1,2,7} PENGWEI HUANG,¹ CLAUDIO CONTI,^{1,3,4} ZHITENG WANG,^{1,2} YONGHUA HU,⁵ DAJUN LEI,⁶ YING LI,^{1,*} AND DIANYUAN FAN¹

¹*SZU-NUS Collaborative Innovation Center for Optoelectronic Science & Technology, International Collaborative Laboratory of 2D Materials for Optoelectronic Science & Technology, Key Laboratory of Optoelectronic Devices and Systems of Ministry of Education and Guangdong Province, College of Optoelectronic Engineering, Shenzhen University, Shenzhen 518060, China*

²*College of Physics and Electronic Engineering, Hengyang Normal University, Hengyang 421002, China*

³*Institute for Complex Systems (ISC-CNR), Via dei Taurini 19, 00185, Rome, Italy*

⁴*Department of Physics, University Sapienza, Piazzale Aldo Moro 5, 00185, Rome, Italy*

⁵*School of Computer Science and Engineering, Hunan University of Science and Technology, Xiangtan 411201, China*

⁶*School of Electronic Information and Electrical Engineering, Xiangnan University, Chenzhou 423000, China*

⁷*zhanglifufu68@hotmail.com*

**queenly@szu.edu.cn*

Abstract: The propagation of decelerating Airy pulses in non-instantaneous cubic medium is investigated both theoretically and numerically. In a Debye model, at variance with the case of accelerating Airy and Gaussian pulses, a decelerating Airy pulse evolves into a single soliton for weak and general non-instantaneous response. Airy pulses can hence be used to control soliton generation by temporal shaping. The effect is critically dependent on the response time, and could be used as a way to measure the Debye type response function. For highly non-instantaneous response, we theoretically find a decelerating Airy pulse is still transformed into Airy wave packet with deceleration. The theoretical predictions are confirmed by numerical simulations.

© 2017 Optical Society of America

OCIS codes: (190.0190) Nonlinear optics; (190.4370) Nonlinear optics, fibers; (190.3270) Kerr effect.

References and links

1. M. V. Berry and N. L. Balazs, "Nonspreading wave packets," *Am. J. Phys.* **47**(3), 264–267 (1979).
2. G. A. Siviloglou and D. N. Christodoulides, "Accelerating finite energy Airy beams," *Opt. Lett.* **32**(8), 979–981 (2007).
3. G. A. Siviloglou, J. Broky, A. Dogariu, and D. N. Christodoulides, "Observation of accelerating Airy beams," *Phys. Rev. Lett.* **99**(21), 213901 (2007).
4. J. Broky, G. A. Siviloglou, A. Dogariu, and D. N. Christodoulides, "Self-healing properties of optical Airy beams," *Opt. Express* **16**(17), 12880–12891 (2008).
5. P. Polynkin, M. Kolesik, J. V. Moloney, G. A. Siviloglou, and D. N. Christodoulides, "Curved plasma channel generation using ultraintense Airy beams," *Science* **324**(5924), 229–232 (2009).
6. P. Polynkin, M. Kolesik, and J. Moloney, "Filamentation of femtosecond laser Airy beams in water," *Phys. Rev. Lett.* **103**(12), 123902 (2009).
7. J. Baumgartl, M. Mazilu, and K. Dholakia, "Optically mediated particle clearing using Airy wavepackets," *Nat. Photonics* **2**(11), 675–678 (2008).
8. P. Zhang, J. Prakash, Z. Zhang, M. S. Mills, N. K. Efremidis, D. N. Christodoulides, and Z. Chen, "Trapping and guiding microparticles with morphing autofocusing Airy beams," *Opt. Lett.* **36**(15), 2883–2885 (2011).
9. T. Vetteburg, H. I. Dalgarno, J. Nylk, C. Coll-Lladó, D. E. Ferrier, T. Čížmár, F. J. Gunn-Moore, and K. Dholakia, "Light-sheet microscopy using an Airy beam," *Nat. Methods* **11**(5), 541–544 (2014).
10. S. Jia, J. C. Vaughan, and X. Zhuang, "Isotropic three-dimensional super-resolution imaging with a self-bending point spread function," *Nat. Photonics* **8**(4), 302–306 (2014).
11. P. Rose, F. Diebel, M. Boguslawski, and C. Denz, "Airy beam induced optical routing," *Appl. Phys. Lett.* **102**(10), 101101 (2013).
12. D. Abdollahpour, S. Sunstov, D. G. Papazoglou, and S. Tzortzakis, "Spatiotemporal airy light bullets in the linear and nonlinear regimes," *Phys. Rev. Lett.* **105**(25), 253901 (2010).

13. A. Chong, W. Renninger, D. N. Christodoulides, and F. W. Wise, "Airy-Bessel wave packets as versatile linear light bullets," *Nat. Photonics* **4**(2), 103–106 (2010).
14. P. Panagiotopoulos, D. G. Papazoglou, A. Couairon, and S. Tzortzakis, "Sharply autofocused ring-Airy beams transforming into non-linear intense light bullets," *Nat. Commun.* **4**, 2622 (2013).
15. I. Kaminer, Y. Lumer, M. Segev, and D. N. Christodoulides, "Causality effects on accelerating light pulses," *Opt. Express* **19**(23), 23132–23139 (2011).
16. R. Driben, Y. Hu, Z. Chen, B. A. Malomed, and R. Morandotti, "Inversion and tight focusing of Airy pulses under the action of third-order dispersion," *Opt. Lett.* **38**(14), 2499–2501 (2013).
17. S. Wang, D. Fan, X. Bai, and X. Zeng, "Propagation dynamics of Airy pulses in optical fibers with periodic dispersion modulation," *Phys. Rev. A* **89**(2), 023802 (2014).
18. I. M. Besieris and A. M. Shaarawi, "Accelerating Airy wave packets in the presence of quadratic and cubic dispersion," *Phys. Rev. E Stat. Nonlin. Soft Matter Phys.* **78**(4), 046605 (2008).
19. Y. Fattal, A. Rudnick, and D. M. Marom, "Soliton shedding from Airy pulses in Kerr media," *Opt. Express* **19**(18), 17298–17307 (2011).
20. L. Zhang, J. Zhang, Y. Chen, A. Liu, and G. Liu, "Dynamic propagation of finite-energy Airy pulses in the presence of higher-order effects," *J. Opt. Soc. Am. B* **31**(4), 889–897 (2014).
21. Y. Hu, M. Li, D. Bongiovanni, M. Clerici, J. Yao, Z. Chen, J. Azaña, and R. Morandotti, "Spectrum to distance mapping via nonlinear Airy pulses," *Opt. Lett.* **38**(3), 380–382 (2013).
22. L. Zhang, H. Zhong, Y. Li, and D. Fan, "Manipulation of Raman-induced frequency shift by use of asymmetric self-accelerating Airy pulse," *Opt. Express* **22**(19), 22598–22607 (2014).
23. C. Ament, P. Polynkin, and J. V. Moloney, "Supercontinuum generation with femtosecond self-healing Airy pulses," *Phys. Rev. Lett.* **107**(24), 243901 (2011).
24. C. Ament, M. Kolesik, J. Moloney, and P. Polynkin, "Self-focusing dynamics of ultraintense Airy waveforms in water," *Phys. Rev. A* **86**(4), 043842 (2012).
25. L. Zhang and H. Zhong, "Modulation instability of finite energy Airy pulse in optical fiber," *Opt. Express* **22**(14), 17107–17115 (2014).
26. Y. Hu, A. Tehranchi, S. Wabnitz, R. Kashyap, Z. Chen, and R. Morandotti, "Improved intrapulse raman scattering control via asymmetric airy pulses," *Phys. Rev. Lett.* **114**(7), 073901 (2015).
27. Y. Zhang, M. Belić, Z. Wu, H. Zheng, K. Lu, Y. Li, and Y. Zhang, "Soliton pair generation in the interactions of Airy and nonlinear accelerating beams," *Opt. Lett.* **38**(22), 4585–4588 (2013).
28. L. Zhang, K. Liu, H. Zhong, J. Zhang, Y. Li, and D. Fan, "Effect of initial frequency chirp on Airy pulse propagation in an optical fiber," *Opt. Express* **23**(3), 2566–2576 (2015).
29. L. Zhang, K. Liu, H. Zhong, J. Zhang, Y. Hu, J. Deng, D. Lei, Y. Li, and D. Fan, "Discriminating the role of Raman effects in the propagation of decelerating and accelerating Airy pulses by time–frequency analysis," *J. Opt.* **18**(1), 015505 (2016).
30. L. Zhang, K. Liu, H. Zhong, J. Zhang, J. Deng, Y. Li, and D. Fan, "Engineering deceleration and acceleration of soliton emitted from Airy pulse with quadratic phase modulation in optical fibers without high-order effects," *Sci. Rep.* **5**, 11843 (2015).
31. J. A. Giannini and R. I. Joseph, "The role of the second Painleve transcendent in nonlinear optics," *Phys. Lett. A* **141**(8–9), 417–419 (1989).
32. S. Jia, J. Lee, J. W. Fleischer, G. A. Siviloglou, and D. N. Christodoulides, "Diffusion-trapped Airy beams in photorefractive media," *Phys. Rev. Lett.* **104**(25), 253904 (2010).
33. I. Kaminer, M. Segev, and D. N. Christodoulides, "Self-accelerating self-trapped optical beams," *Phys. Rev. Lett.* **106**(21), 213903 (2011).
34. A. Lotti, D. Faccio, A. Couairon, D. G. Papazoglou, P. Panagiotopoulos, D. Abdollahpour, and S. Tzortzakis, "Stationary nonlinear Airy beams," *Phys. Rev. A* **84**(2), 021807 (2011).
35. R. Bekenstein and M. Segev, "Self-accelerating optical beams in highly nonlocal nonlinear media," *Opt. Express* **19**(24), 23706–23715 (2011).
36. I. Dolev, I. Kaminer, A. Shapira, M. Segev, and A. Arie, "Experimental observation of self-accelerating beams in quadratic nonlinear media," *Phys. Rev. Lett.* **108**(11), 113903 (2012).
37. I. Kaminer, J. Nemirovsky, and M. Segev, "Self-accelerating self-trapped nonlinear beams of Maxwell's equations," *Opt. Express* **20**(17), 18827–18835 (2012).
38. M. Bache, O. Bang, J. Moses, and F. W. Wise, "Nonlocal explanation of stationary and nonstationary regimes in cascaded soliton pulse compression," *Opt. Lett.* **32**(17), 2490–2492 (2007).
39. C. Conti, S. Stark, P. St. J. Russell, and F. Biancalana, "Multiple hydrodynamical shocks induced by the Raman effect in photonic crystal fibers," *Phys. Rev. A* **82**(1), 013838 (2010).
40. G. P. Agrawal, *Nonlinear Fiber Optics*, 4 ed. (Academic Press, 2007).
41. E. E. Serebryannikov, C. Rivero, R. Stegeman, and A. M. Zheltikov, "Soliton transients and supercontinuum generation in high-Raman-gain materials," *J. Opt. Soc. Am. B* **24**(1), 137–141 (2007).
42. R. Zhang, J. Teipel, and H. Giessen, "Theoretical design of a liquid-core photonic crystal fiber for supercontinuum generation," *Opt. Express* **14**(15), 6800–6812 (2006).
43. M. Vieweg, T. Gissibl, S. Pricking, B. T. Kuhlmeier, D. C. Wu, B. J. Eggleton, and H. Giessen, "Ultrafast nonlinear optofluidics in selectively liquid-filled photonic crystal fibers," *Opt. Express* **18**(24), 25232–25240 (2010).

44. S. Pricking and H. Giessen, "Generalized retarded response of nonlinear media and its influence on soliton dynamics," *Opt. Express* **19**(4), 2895–2903 (2011).
45. R. V. J. Raja, A. Husakou, J. Hermann, and K. Porsezian, "Supercontinuum generation in liquid-filled photonic crystal fiber with slow nonlinear response," *J. Opt. Soc. Am. B* **27**(9), 1763–1768 (2010).
46. J. A. Fleck, Jr. and P. L. Kelley, "Temporal aspects of the self-focusing of light beams," *Appl. Phys. Lett.* **15**(10), 313–315 (1969).
47. J. A. Fleck, Jr. and R. L. Carman, "Effect of relaxation on small-scale filament formation by ultrashort light pulses," *Appl. Phys. Lett.* **20**(8), 290–293 (1972).
48. L. Zhang, S. Wen, X. Fu, J. Deng, J. Zhang, and D. Fan, "Spatiotemporal instability in dispersive nonlinear Kerr medium with a finite response time," *Opt. Commun.* **283**(10), 2251–2257 (2010).
49. B. Kibler, C. Michel, J. Garnier, and A. Picozzi, "Temporal dynamics of incoherent waves in noninstantaneous response nonlinear Kerr media," *Opt. Lett.* **37**(13), 2472–2474 (2012).
50. C. Conti, M. A. Schmidt, P. St. J. Russell, and F. Biancalana, "Highly noninstantaneous solitons in liquid-core photonic crystal fibers," *Phys. Rev. Lett.* **105**(26), 263902 (2010).
51. F. Deng, W. Hong, and D. Deng, "Airy-type solitary wave in highly noninstantaneous Kerr media," *Opt. Express* **24**(14), 15997–16002 (2016).

1. Introduction

Finite energy Airy beam, solutions to the free-particle Schrödinger equation [1], was first introduced theoretically [2] and later realized experimentally [3] by Christodoulides and associates in 2007. These results attracted considerable attention because of the evidence of self-acceleration, self-healing and quasi-diffraction-free [2–4]. Airy beams trigger many applications, including the formation of curved filamentation [5, 6], the manipulation of micro particles [7, 8], high-resolution microscopy [9, 10], all-optical routing [11], and the generation of spatiotemporal light bullets [12–14]. Also in the temporal domain, Airy pulses were studied theoretically [2, 3] and experimentally [12, 13]. The self-bending trajectory of Airy beams in the spatial domain turns into a *self-accelerating* or *self-decelerating* dynamics for temporal Airy pulses. The dynamics is controlled by the shape of the pulse profile [15] and many researchers investigate the possible applications in pulse transmission [15–30].

Airy wave packets are non-spreading solutions in the linear regime. One expects that nonlinear effects may deform and destroy these wave-packets [19]. However, Giannini and Joseph derived temporal self-accelerating solutions in nonlinear Kerr media as early as 1989. These solutions are given in terms of Painlevé transcendents of second type [31]. Other authors also demonstrated self-trapped Airy beams in nonlinear media with different kinds of nonlinearity [32–37]. In particular, Bekenstein *et al.* considered self-accelerating beams in highly nonlocal nonlinear optical media, in which boundary conditions strongly affect propagation dynamics [35]. In analogy to spatial nonlocal media, a non-instantaneous response as the Raman effect leads to several interesting phenomena in temporal domain [38, 39]. The Raman effect is largely enhanced with respect to silica glass fibers [40] by considering materials as tellurite glasses [41]. In addition, the recently developed photonic crystal fibers filled with molecular liquids offer an unprecedented platform highly non-instantaneous nonlinear optics [42–45]. The non-instantaneous nonlinear response alters self-focusing of light beam [46, 47], spatiotemporal modulation instability [48], the formation of temporal incoherent solitons [49], and solitons [50].

Prior studies on temporally nonlocal nonlinearity mostly considered pulses with symmetric profiles as hyperbolic secant and Gaussian pulses. Airy pulses have an asymmetric profile with rapidly oscillating tails and complex propagation dynamics [15–30]. We expect that the asymmetry of Airy pulses may lead to fairly non-trivial dynamics because of the time-asymmetric response function of non-instantaneous media that derives from causality [15]. Exploring asymmetric pulses in combination with the non-instantaneous nonlinearity may open new interesting perspective in pulse shaping and in the control of highly nonlinear processes as supercontinuum generation. As shown by Deng *et al.*, Airy-type solitary waves are generated by *accelerating Airy pulse* in the highly non-instantaneous Kerr media [51]. A very intriguing possibility however is given by the *decelerating Airy pulses* as these may counteract the retarded action of the nonlinearity. Loosely speaking one may expect that if the

pulse reduces its velocity and its tails propagate in front of the main lobe, its main lobe becomes synchronous with nonlinearity induced by the retarded nonlinear response and ultimately the medium behaves as an instantaneous medium.

In the present work we will investigate the propagation dynamics of decelerating Airy pulse in a medium with non-instantaneous Kerr nonlinear response in which the nonlinear contribution to the refractive index is governed by a relaxing Debye type equation. We study the effect of the response time and demonstrate that in critical conditions the retarded nonlinearity and the deceleration develop and change simultaneously as well as generate an accelerated soliton with negative acceleration.

2. Theoretical model

We consider the nonlinear Schrödinger equation accounting for a Debye type relaxation effect, which is written in the following dimensionless form [49, 50]

$$i \frac{\partial U}{\partial Z} + \frac{1}{2} s \frac{\partial^2 U}{\partial T^2} + \sigma N^2 U \int_{-\infty}^{+\infty} R(T-T') |U(T')|^2 dT' = 0. \quad (1)$$

Here, the field amplitude $U(T, Z)$ is normalized such that its peak is equal 1. $R(T) \equiv \Theta(T)h(T)$ is the response function with $h(T) = \exp(-T/T_r)/T_r$, $T_r = t_r/t_0$, $\Theta(t)$ is the Heaviside function (zero for $T < 0$ and unity for $T > 0$), t_r and t_0 are the response time and the pulse width. The other dimensionless variables are defined as

$$T = \frac{t - z/v_g}{t_0}, Z = \frac{z}{L_D}, N = \sqrt{\gamma P_0 L_D}, s = \text{sgn}(\beta_2), \sigma = \text{sgn}(\gamma). \quad (2)$$

Where P_0 is the peak power of input pulse, v_g is the group velocity, γ is nonlinear parameter, $L_D = t_0^2/|\beta_2|$ is the dispersion length, β_2 is the group-velocity dispersion. $s = -1$ ($s = +1$) represents normal (anomalous) dispersion, $\sigma = -1$ ($\sigma = +1$) denotes defocusing (focusing) nonlinearity.

The initial decelerating Airy pulse is $U(T, 0) = f(a) \text{Ai}(T) \exp(aT)$ with $0 < a < 1$. $f(a)$ keeps the maximum amplitude of initially launched pulse to 1 for any values of a . We use the standard split-step Fourier method to numerically solve Eq. (1) [40].

3. Theoretical results

Based on the method used in [50], as $T_r \gg 1$, Eq. (1) can be written as

$$i \frac{\partial U}{\partial Z} + \frac{s}{2} \frac{\partial^2 U}{\partial T^2} + \sigma R(T)U = 0. \quad (3)$$

For $T < 0$, $R(T) = 0$, Eq. (3) is reduced as follows

$$i \frac{\partial U}{\partial Z} + \frac{s}{2} \frac{\partial^2 U}{\partial T^2} = 0. \quad (4)$$

Its solution can be written as

$$U(Z, T) = \text{Ai} \left(T - \frac{Z^2}{4} + isa_1 Z \right) \exp \left[a_1 \left(T - \frac{Z^2}{2} \right) - \frac{is^3 Z^3}{12} + i \frac{sa_1^2 Z}{2} + i \frac{sTZ}{2} \right]. \quad (5)$$

For $T > 0$, we have $R = E/T_r$ independent of T , and neglect all other terms. Equation (3) becomes

$$i \frac{\partial U}{\partial Z} + \frac{s}{2} \frac{\partial^2 U}{\partial T^2} + \frac{\sigma E}{T_r} U = 0. \quad (6)$$

Where $E = N^2 \int_{-\infty}^{\infty} |U(T')|^2 dT'$ is proportional to the total power of photons launched into the fiber. The solution of Eq. (6) reads

$$U(Z, T) = Ai \left(T - \frac{Z^2}{4} + isa_2 Z \right) \exp \left[a_2 \left(T - \frac{Z^2}{2} \right) - \frac{is^3 Z^3}{12} + i \frac{sa_2^2 Z}{2} + i \frac{sTZ}{2} + i \frac{\sigma EZ}{T_r} \right]. \quad (7)$$

Note that this solution has a truncation coefficient a_2 which is different from a_1 in Eq. (5), and there is the additional phase factor (nonlinear phase) $\sigma E/T_r$. However, these two solutions must match at $T = 0$, the phase factors must match and hence we have

$$\frac{sa_1^2}{2} = \frac{sa_2^2}{2} + \frac{\sigma E}{T_r} + 2n\pi. \quad (8)$$

This equation has a number of consequences: As there are many solutions (varying $n = 0, 1, 2, \dots$) one can have multiple Airy pulses for $T > 0$ with different a_2 coefficient; The ground state solution will exist only if a_2 is positive, and this implies some critical values; With the phase-matching condition we also have an amplitude matching, but this is assumed to be an higher order effect that implies some changes in the amplitudes with respect the linear Airy beams.

It can be obtained from Eq. (8) that the existence condition of fundamental solution $n = 0$ is

$$\frac{a_2^2}{2} = \frac{a_1^2}{2} - \frac{s\sigma E}{T_r} > 0, \quad (9)$$

which implies that for $s\sigma < 0$ one always has a solution. On the contrary for $s\sigma > 0$ a solution only exist if

$$\frac{a_1^2}{2} \geq \frac{E}{T_r}. \quad (10)$$

It implies critical values for T_r and E , thus for the critical values is

$$\left(\frac{E}{T_r} \right)_{cr} = \frac{a_1^2}{2}. \quad (11)$$

It should be noted from Eq. (9) that a_2 is zero when E and T_r satisfy the Eq. (11). Then Eq. (7) represents infinite energy Airy pulse.

4. Numerical results

Figure 1 shows the propagation dynamics of decelerating Airy pulse with $a = 0.03$ and $N = 2$ as a function of propagation distance in non-instantaneous nonlinear focusing Kerr medium with different response time T_r and anomalous dispersion. This corresponds to

$s\sigma > 0$. Figure 1 shows that the propagation dynamics of decelerating Airy pulse vary with the value of response time T_r . Figure 1(a) shows the case $T_r = 0$, in which the nonlinearity is instantaneous response [19, 20]. In this case, the main lobe of decelerating Airy pulse is able to shed soliton. The shedding soliton undergoes successive collision with the other decelerating side lobes, and then becomes stable. Due to the self-healing property of Airy pulse, the rest of decelerating Airy pulse reconstructs a new Airy pattern. The propagation dynamic of decelerating Airy pulse changes drastically when $T_r \neq 0$. For $T_r = 0.1$, we find three trajectories marked with numbers 1, 2, and 3. Trajectory one originates out of the main lobe with the strongest bending and deceleration. When the response time increases ($T_r=0.5$) trajectories 2 and 3 merge with periodically oscillations. The curvature of trajectory 1 becomes smaller compared to that in Fig. 1(b). For T_r in the range from 2.0 to 4.0, all trajectories merge become stable. For even larger values of T_r , see Fig. 1(f), such stable dynamics is broken down, manifesting the peak intensity decreases. These propagation dynamics are very similar to that of linear propagation of decelerating Airy pulse [2, 3].

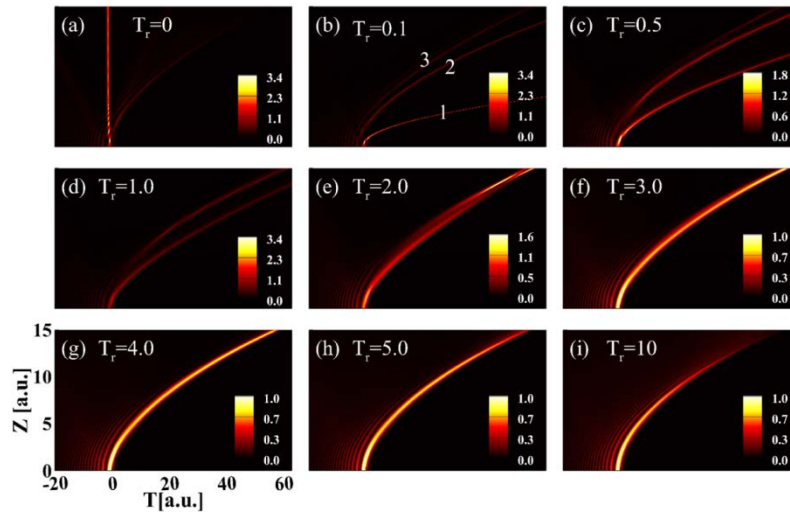


Fig. 1. Temporal evolution of decelerating Airy pulse with $a = 0.03$ in non-instantaneous Kerr nonlinear medium with $N = 2$ and different response time T_r .

Figure 1 shows that there is a critical value of response time for the formation of stable Airy-like dynamics under the fixed value of N . For $N = 2$ and $a = 0.03$, the critical value of T_r is about 4. We carried out a series of numerical experiments for observing the stable Airy-like dynamics by varying the response time T_r and the nonlinear parameter N . The corresponding numerical results are shown in Fig. 2. Figure 3(a) shows the dependence of the critical values of response time T_r^c on the parameter N . As N is increased, the nonlinear contribution is enhanced. But nonlinearity decrease with an increase T_r . By choosing suitable values of T_r and N , their contributions will be counteracted. This trend can also be found from Eq. (11).

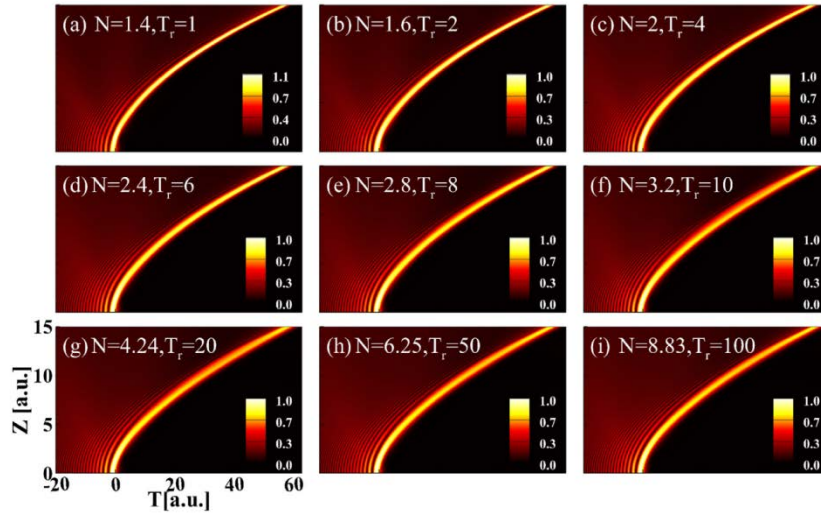


Fig. 2. Stable temporal evolution of decelerating Airy pulse with $a = 0.03$ in non-instantaneous Kerr nonlinear medium with different response time T_r and nonlinearity N .

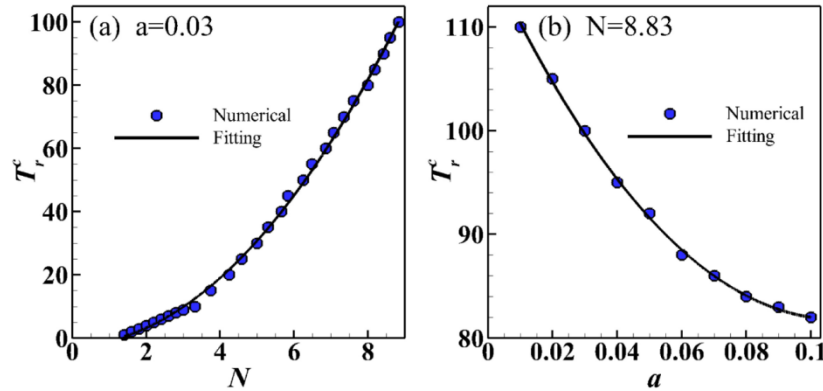


Fig. 3. The critical values of the response time T_r^c is plotted as a function of (a) nonlinearity N and (b) the truncation coefficient a .

The truncation coefficient a also determines the unique features of decelerating Airy pulse [2, 3]. Figure 4 shows the impact of truncation coefficient on the propagation dynamics of decelerating Airy pulse in non-instantaneous nonlinear Kerr medium with $T_r = 4$ and $N = 2$. When a is below 0.03, the main lobe not only becomes stable but also contains more power. For $a > 0.03$, [Figs. 4(g)-4(i)], the main lobe first undergoes an initial reshaping phase in the first two propagation distances. Also the main lobe peak intensity decreases. As was seen in Fig. 4, there is a critical value of truncation coefficient for the formation of stable peak intensity. The relationship between the critical values of response time and the truncation coefficient a for $N = 8.83$ is shown in Fig. 3(b). These findings may be justified by recalling that the total power of decelerating Airy pulse is given by $E_{total} = \sqrt{1/8\pi a} \exp(2a^3/3)$ [2] and increases with a , hence N must scale accordingly to maintain the value of nonlinearity. This is consistent with the theoretical predictions from Eq. (11).

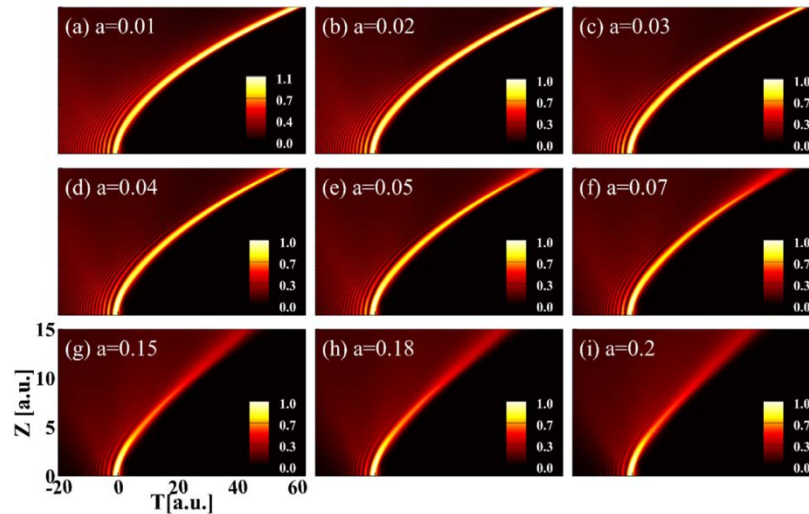


Fig. 4. Temporal evolutions of decelerating Airy pulse with different values of truncation coefficient in non-instantaneous Kerr nonlinear medium with the parameters $T_r = 4$ and $N = 2$.

In the limit of a highly temporal nonlocal response, where $R(T)$ is much broader than the intensity profile, the theoretical results presented in Sec. 3 indicate the shape of Airy pulse is unchanged during the propagation. To verify these theoretical predictions, we simulated the propagation dynamics of decelerating Airy pulse with $a = 0.03$ and $N = 2$ in highly non-instantaneous cubic media, shown in Figs. 5(a)-5(c). In these three cases, the propagation processes are almost same. They should be compared with Fig. 5(d) where the case of linear propagation of decelerating Airy pulse is shown. There are no differences between the decelerating Airy pulse propagation in highly non-instantaneous media and that in linear media. This is very agreement with the theoretical predictions obtained from Eq. (7). For $a = 0.03$ and $N = 2$, one yields $E \approx 7.0$. Therefore, the larger T_r , the smaller E/T_r . And such that a_2 is very close to a_1 . This means that the evolution of decelerating Airy pulse in highly non-instantaneous cubic media is almost same as that in linear dispersive media. We also check the peak intensity and the corresponding position as a function of the propagation distance. The results are shown in Figs. 5(e) and 5(f). It is clearly seen from Figs. 5(e) and 5(f) that the all curves are overlapping. The theoretical results from Eq. (7) are confirmed by numerical simulations once again.

In order to clarify the novel behavior observed in Fig. 2 especially due to the decelerating nature of the incident pulse, Fig. 6 depicts the accelerating Airy pulse propagation in highly non-instantaneous cubic media with the same parameter values used in Figs. 2(a)-2(c). This results should be compared with Figs. 2(a)-2(c) where the case of a decelerating pulse is shown. The differences between the two can be attributed to the acceleration and deceleration of the input pulse, which depending on whether the tail orientation is in front of or behind the main lobe. For the case of accelerating Airy pulse, Fig. 6 shows a part of energy is shed from the main lobe, and form a well-resolved prominent spike. The intensity of spike decreases with an increasing T_r . Although such spike collides with side lobes, the rest of the accelerating Airy pulse continues to accelerate owing to its unique properties of self-accelerating and self-healing.

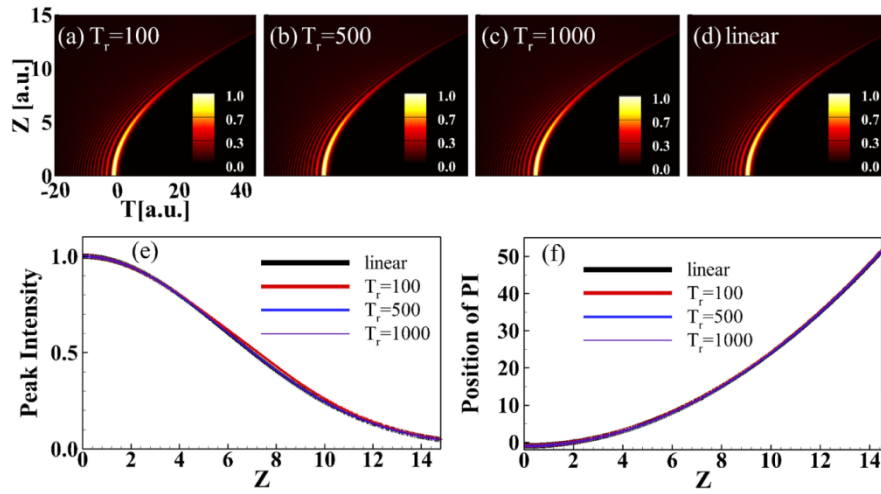


Fig. 5. Temporal evolution of decelerating Airy pulse with $a = 0.03$ and $N=2$ in (a-c) highly non-instantaneous cubic media and (d) linear media. The corresponding (e) Peak intensity (PI) and (f) position of PI as a function of propagation distance.

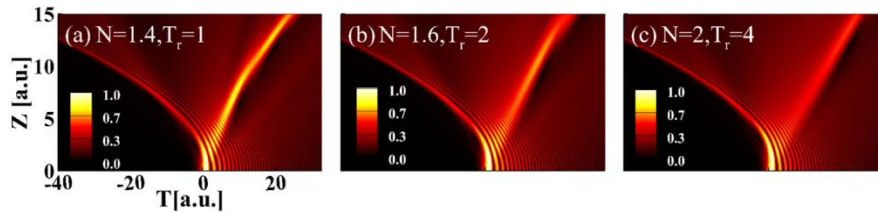


Fig. 6. Temporal evolution of accelerating Airy pulse with $a = 0.03$ in non-instantaneous Kerr nonlinear medium with different response time T_r and nonlinearity N .

We track the nonlinear, intensity-dependent additive to the refractive index $\delta n(T, Z) = \int_{-\infty}^{+\infty} \exp(T' - T/T_r)/T_r |U(T', Z)|^2 dT'$ during the nonlinear propagation in order to gain more physical insights. For the instantaneous case, $\delta n(T, Z) = |U(T', Z)|^2$, manifesting that the nonlinear refractive changes simultaneously with the pulse. Figure 7 shows the evolution of δn when accelerating and decelerating pulses propagate in non-instantaneous cubic media with $N = 2$ and $T_r = 4$. Figure 7(a) indicates the accelerating Airy pulse has a force to counteract the retarded nonlinearity. As a result, the non-instantaneous nonlinearity decrease quickly after about 4 propagation distances. However, the decelerating Airy pulse is synchronous with the retarded nonlinearity, see Fig. 7(b). Consequently, a stable potential well is formed to support an accelerated soliton because the deceleration of pulse compensates the retarded nonlinearity. The reason can be understood by recalling the self-healing and accelerating properties. For the purpose of facilitating self-healing, the energy flux of Airy pulse from the side lobes towards the main lobe [2], leading to a curvature of the trajectory of the main lobe. On the other hand, in the anomalous-dispersion regime low-frequency (red-shifted) components of an optical pulse travel slower than high-frequency (blue-shifted) of the same pulse [40]. During the linear propagation, therefore, the main lobe of accelerating Airy pulse only contains the high-frequency (blue-shifted) components, while the main lobe of decelerating Airy pulse has the low-frequency (red-shifted) components. This difference between accelerating and decelerating Airy pulse is clearly observed by using time-frequency analysis [29]. The retarded response is able to accumulate the nonlinearity to

the trailing edge of the pulse. As a consequence, the main lobe of decelerating Airy pulse experiences larger nonlinearity than that of accelerating one, resulting in the formation of soliton with deceleration.

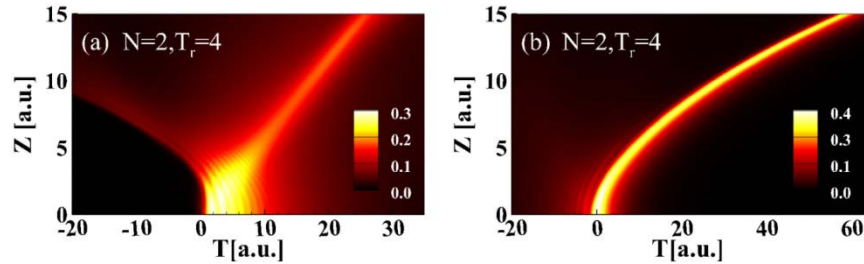


Fig. 7. The change of nonlinear refractive $\delta n(T, Z)$ as a function of propagation distance for (a) accelerating and (b) decelerating Airy pulses propagation in non-instantaneous Kerr nonlinear medium.

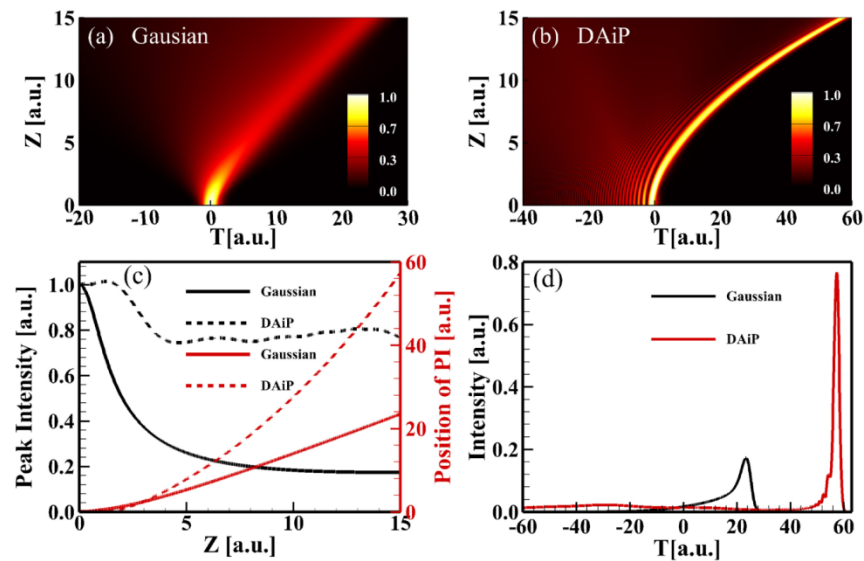


Fig. 8. Temporal evolution of (a) Gaussian pulse and (b) decelerating Airy pulse (DAiP) with $\alpha = 0.03$ in non-instantaneous nonlinear medium. (c) Peak intensity (PI) and the position of PI along propagation. (d) Output pulse shapes at $Z = 15$.

Figure 8(a) shows the temporal evolution of Gaussian pulse as a function of the propagation distance in non-instantaneous response nonlinear Kerr medium with $T_r = 4$ and $N = 2$. From the comparison with the decelerating Airy beams, we see that a Gaussian pulse shows a weak peak with a long pedestal displays slow deceleration. These difference are also evident in Fig. 8(c) and 8(d). For a Gaussian pulse propagation, in Fig. 8(c), the peak intensity decreases with an increase in the propagation distance. For decelerating Airy pulse propagation, the peak intensity remains almost unchanged in first 1.8 propagation distances, then decreases with an increasing propagation distance in the range of $1.8 < Z < 4$; with further increasing propagation distance, the peak intensities are almost unchanged. That indicates the peak intensity enhancement after first four propagation distances. The intensity enhancement of the main lobe is illustrated in Fig. 8(d) where the output pulse profile is compared with the Gaussian case. The Gaussian input is completely destroyed with a long tail and weak peak intensity. The position of peak intensity corresponding to the trajectory of the

main lobe is also shown in Fig. 8(c) as a function of propagation distance Z . In the first three propagation distances, their peak intensity positions always remain the same. With further increase the propagation distances, the amount self-deceleration of the main lobe of Airy pulse propagation is larger than that of Gaussian pulse propagation. This process is very different from that in instantaneous response Kerr medium in which the Airy pulse emits soliton [19–21].

5. Conclusion

In summary, we have studied the impact of finite nonlinear response time of Kerr medium on the decelerating Airy pulse propagation. We found that, for weak and general Debye type non-instantaneous response, the non-instantaneous Kerr nonlinearity can be used to control decelerating Airy pulse propagation, leading to trajectory reshaping and enhancement of the main lobe intensity. The main lobe of decelerating Airy pulse evolves to form a single intensity-enhanced soliton with deceleration, this does not occur for accelerating Airy and Gaussian input pulses. Small truncation coefficient is helpful for the formation of decelerating intensified main lobe. We determined the dependence of the critical values of response time on the truncation coefficients and input peak power of decelerating Airy pulse for the accelerated soliton formation. For highly non-instantaneous response, we have theoretically found the decelerating Airy pulse still exhibits Airy wave packet with different acceleration. These results may prove useful for manipulating and exploiting various important applications of decelerating Airy pulse.

Funding

National Natural Science Foundation of China (Grant Nos. 61505116, 61575127, 61308001, 61605044), the Natural Science Foundation of Guangdong Province (Grant No. 2016A030313049), the Natural Science Foundation of SZU (Grant No. 000053), the Science and Technology Planning Project of Guangdong Province (Grant No. 2016B050501005), the open foundation of the Hunan Provincial Applied Basic Research Base of Optoelectronic Information Technology of Hengyang Normal University (Grant No. GD16K01), China Postdoctoral Science Foundation (2016T90797), and the Aid Program for Science and Technology Innovative Research Team in Higher Educational Institutions of Hunan Province, CC acknowledges the John Templeton Foundation (Grant No. 58277)

Acknowledgment

We thank the referees for their enlightening comments to improve the paper.